Mongolian Geoscientist

Original Article

Climate and Topographic Controls on Paleo-Drainage Network Evolution in Semi-Arid Eastern Mongolia

Batzorig Batbold[1,2]*, Ulambadrakh Khukhuudei[2,3], Altanbold Enkhbold[4]*

[1]*Wildlife Science and Conservation Center of Mongolia, Ulaanbaatar 14230, Mongolia*
[2]*Research Center of Geology and Mineral Resources, School of Arts and Sciences, National University of Mongolia, Ulaanbaatar 14200, Mongolia*
[3]*Center for Global Tectonics, School of Earth Sciences and State Key Laboratory for Geological Processes and Mineral Resources, China University of Geosciences, Wuhan 430074, China*
[4]*Laboratory of Geopedology, Department of Geography, School of Arts and Sciences, National University of Mongolia, Ulaanbaatar 14200, Mongolia*

**Corresponding author:* altanbold@num.edu.mn, 25d1num0224@stud.num.edu.mn, *ORCID:* 0000-0002-5195-5558, 0000-0003-3810-449X

ARTICLE INFO

Article history:

Received: 25 March, 2026
Revised: 10 June, 2026
Accepted: 25 June, 2026

ABSTRACT

This study reconstructs paleo-drainage basins in Eastern Mongolia using Digital Elevation Models -based geomorphological analysis and compares their morphometric and environmental characteristics with those of modern river basins. Two major paleo-drainage systems were identified, originating from the Greater Khingan Mountains, Nukht Davaa, and the Dariganga Volcanic Plateau, and forming extensive networks of shallow valleys and interconnected lacustrine basins. Morphometric analysis indicates that these paleo-basins exhibit lower slopes, reduced local relief, and more planar surfaces than active basins, suggesting reduced hydrological efficiency and potentially limited capacity to sustain perennial flow under present climatic conditions. Environmental indicators, including precipitation, Normalized Difference Vegetation Index, Land Surface Temperature, and Evapotranspiration, show that paleo-basins are largely located in low-precipitation, low-relief areas, reinforcing the inference of limited water supply. Comparison with regional paleoclimate records indicates that humid conditions during the mid-late MIS 3 period (~43,800-29,500 cal BP) likely supported more extensive hydrological networks, whereas increasing aridity during MIS 2 and the Holocene contributed to reduced flows and system fragmentation. The results demonstrate that paleo-drainage evolution in semi-arid Eastern Mongolia is governed by climate-driven hydrological thresholds interacting with topographic constraints. The findings highlight the importance of non-linear hydrological responses to climatic variability, particularly in low-relief semi-arid systems. This study provides a process-based framework for understanding hydrological disconnection and offers broader implications for paleo-drainage reconstruction across Central and Eastern Asian regions.

Keywords: Paleo-drainage, Quantitative geomorphology, Morphometric analysis, Fluvial system change, River basin

INTRODUCTION

Paleohydrological systems in the arid regions of Central and Eastern Asia have experienced significant changes throughout the Holocene, largely influenced by climatic fluctuations, as indicated by multiple paleoclimate records (Herzschuh, 2006; Chen et al., 2008). Moreover, evidence from aeolian deposits and lacustrine deposits suggests that many of the region's currently dry valleys likely developed under relatively more humid conditions during the early-mid Holocene (Ding et al., 2021).

Eastern Mongolia has experienced alternating phases of hydrological activity and aridity during the Quaternary, largely influenced by climatic variability (Murzaev, 1952; Marinov and Khasin, 1954). During the Early Quaternary, relatively humid climatic conditions facilitated the development of well-defined paleo-drainage networks. However, this phase was not sustained, and relict valleys from these earlier hydrologically active periods remain well preserved in the present landscape (Murzaev, 1952; Marinov and Khasin, 1954). According to Chen et al. (2008), Mongolia experienced humid conditions during the Early Holocene, followed by progressive aridification beginning in the mid-Holocene.

Previous studies by Murzaev (1952) and Tsegmid (1969) indicate that many valleys in Eastern Mongolia are predominantly oriented from southwest to northeast and were previously likely drained toward the Buir Lake and Hulun Lake basins. Murzaev (1952) identified widespread paleo dry channels across the Menen and Buir Lake plains and distinguished two major paleo-fluvial systems originating from the Dariganga Volcanic Plateau and the southwestern Nukht Davaa area. He also noted well-preserved fluvial terraces within these valleys and, based on their geomorphic relationship with the modern drainage network and the accumulative surfaces surrounding Buir Lake, suggested that prolonged hydrological activity may have persisted throughout the early Holocene. These observations indicate that Eastern Mongolia once supported a more extensive and interconnected drainage network than that observed today. Such dry valleys are generally interpreted as remnants of former active hydrological systems that became inactive due to climatic changes, tectonic movements, or variations in hydrological conditions (Schumm, 1977; Bridge, 2003).

The Orshuun River connects Buir Lake and Hulun Lake and was likely part of a single hydrological basin in the past, sharing similar geomorphological origins (Tsegmid, 1969; Enkhbold et al., 2021; Altanbold and Ulambadrakh, 2022).

Key morphometric parameters of drainage basins, including area, length, elevation range, total relief, slope distribution, and longitudinal profiles, are essential for understanding basin evolution, erosion intensity, and equilibrium states (Strahler, 1952; Hack, 1973). Furthermore, the hypsometric integral provides a quantitative measure of landscape development (Strahler, 1957; Willgoose and Hancock, 1998). In recent years, the use of Digital Elevation Models (DEMs) and remote sensing data has significantly advanced geomorphological studies, enabling more accurate extraction of drainage networks and morphometric characteristics (Tarboton, 1997; Farr et al., 2007).

DEM -based morphometric analyses allow for the calculation of parameters such as slope, local relief, and flow accumulation, facilitating a more comprehensive evaluation of basin morphology and hydrological characteristics (Evans, 2012; Pike et al., 2009; Enkhbold et al., 2025a). Additionally, remote sensing-derived datasets-including Normalized Difference Vegetation Index (NDVI), Land Surface Temperature (LST), Evapotranspiration (ET), and precipitation-enable the assessment of contemporary environmental and climatic conditions within drainage basins (Tucker, 1979; Mu et al., 2011; Wan et al., 2015; Fick and Hijmans, 2017). In Mongolia, satellite data and Geographic Information Systems (GIS) are increasingly being applied in hydrological and geomorphological studies (Dorjsuren et al., 2024; Enkhbold et al., 2025a, b; Batzorig et al., 2025).

Previous studies in the study area have largely focused on regional-scale geological and geomorphological mapping (Tomurtogoo et al., 1998; National Atlas of Mongolia, 1990; National Atlas of Mongolia, 2009, 2022; Bayanjargal and Nyamkhuu, 2017). These mapping efforts have identified major tectonic structures, the distribution of Quaternary sediments, and the general characteristics of landforms in Eastern Mongolia. For instance, geological and geomorphological maps at scales ranging from 1:500,000 to 1:3,000,000 have delineated major valleys, depressions, and their geomorphic features within the study area.

However, these studies have not focused in sufficient detail on the origin, evolution, and paleo-drainage connections of individual basins and valley systems at a detailed morphometric scale. Therefore, more comprehensive and spatially explicit investigations are required to better constrain the origin, internal structure, and hydrological connectivity of these landforms. In particular, while previous work has recognized the presence of paleo-drainage remnants in Eastern Mongolia, their basin-scale organization, boundary conditions, and connectivity thresholds remain insufficiently resolved. Moreover, the interactions between morphometric controls and climate-driven hydrological connectivity have rarely been quantified in semi-arid continental basin systems.

Despite previous geomorphological mapping efforts, a process-based and basin-scale understanding of how paleo-drainage networks respond to coupled climatic and topographic controls remains limited. In particular, the role of threshold-driven hydrological connectivity and fragmentation processes in low-relief semi-arid basins has not been systematically evaluated using detailed morphometric approaches.

Accordingly, the main objective of this study is to conduct a detailed basin-scale morphometric analysis of paleo- and modern drainage systems in Eastern Mongolia, to identify previously unrecognized paleo-basins and characterize their internal geomorphic structure, drainage organization, and connectivity conditions. This study further compares these paleo-basins with adjacent active drainage basins in terms of morphometric parameters and contemporary climatic variables. Beyond regional implications, the study contributes to a broader understanding of how semi-arid continental basins evolve under coupled climatic forcing and topographic constraints. The findings provide new insights into threshold-controlled hydrological connectivity and basin fragmentation processes widely observed across Central and Eastern Asian dryland environments.

This study, therefore, focuses on the detailed morphometric characterization of dry valleys and drainage basins in Eastern Mongolia and evaluates their hydrological evolution at the basin scale. In addition, it aims to reconstruct and refine the spatial organization of paleo-drainage networks and associated lake systems through high-resolution geomorphological and GIS -based analyses.

REGIONAL SETTINGS

The study area is located in Eastern Mongolia and extends across the Khentii Mountains, the Greater Khingan Mountains-which spans both Mongolia and China-and the intervening plains (Fig. 1).

The Quaternary tectonic evolution of the Khentii Mountains remains insufficiently studied to date

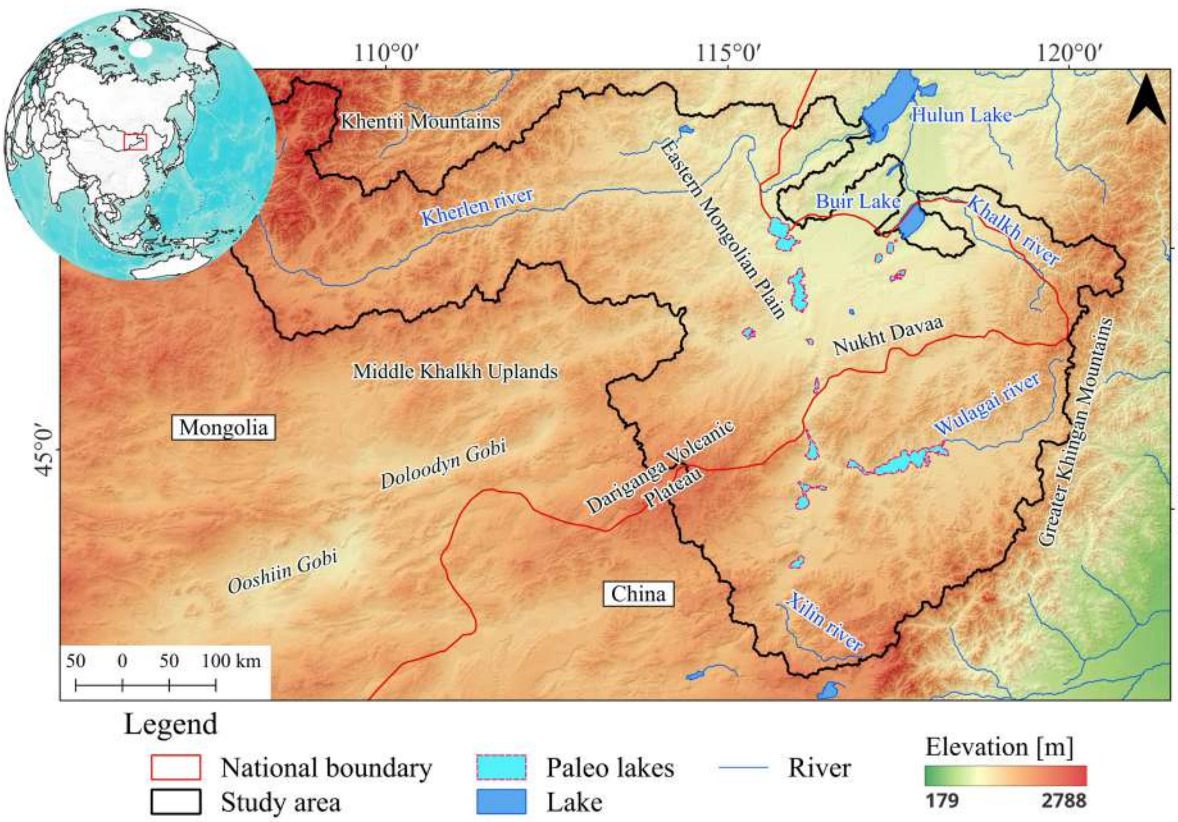

Fig. 1. Location of the study area in eastern Mongolia, showing the distribution of present lakes, reconstructed paleolakes, and major rivers. Elevation is derived from a DEM

(Khukhuudei et al., 2024). Florensov (1978) proposed that the Khentii Mountains formed through differential block uplift and noted relict planation surfaces at various elevations. The broad, arcuate uplift of the Khentii Mountains developed after the Middle Mesozoic and after the closure of the Mongol-Okhotsk Ocean (Tomurtogoo et al., 2005; Jolivet et al., 2017; Arzhannikova et al., 2020; Wang et al., 2022). The range is characterized by flat summits preserving ancient planation surfaces and widespread glacial landforms (Khukhuudei et al., 2024). The mean annual air temperature is below -4°C, and annual precipitation ranges from 300 to 400 mm (Natsagdorj and Gomboluudev, 2017; Yembuu, 2021).

The relatively flat to gently undulating terrain extending from the Khentii Mountains to the foothills of the Greater Khingan Mountains constitute the Eastern Mongolian Plain (Yembuu, 2021). This region is bordered by low to medium-elevation mountains to the west, south, and east, while the northern part is generally flat with occasional low hills and ridges, exhibiting minimal relative relief (Tsegmid, 1969; Jigj, 1975; Khukhuudei et al., 2024). The mean annual air temperature ranges from 0 to 4°C, and annual precipitation ranges from 180 to 280 mm (Natsagdorj and Gomboluudev, 2017; Yembuu, 2021).

The Eastern Mongolian Plain comprises diverse geomorphological units, including accumulative, erosional, structural, and gently undulating hilly terrains (Syrnev, 1982). At the regional scale, erosional plains developed on Paleozoic volcanic and metamorphic rocks, as well as on Early Mesozoic sedimentary and volcanic formations, are distinguished from structural plains formed on Late Cretaceous and Neogene deposits (Ulambadrakh, 2014; Khukhuudei et al., 2024).

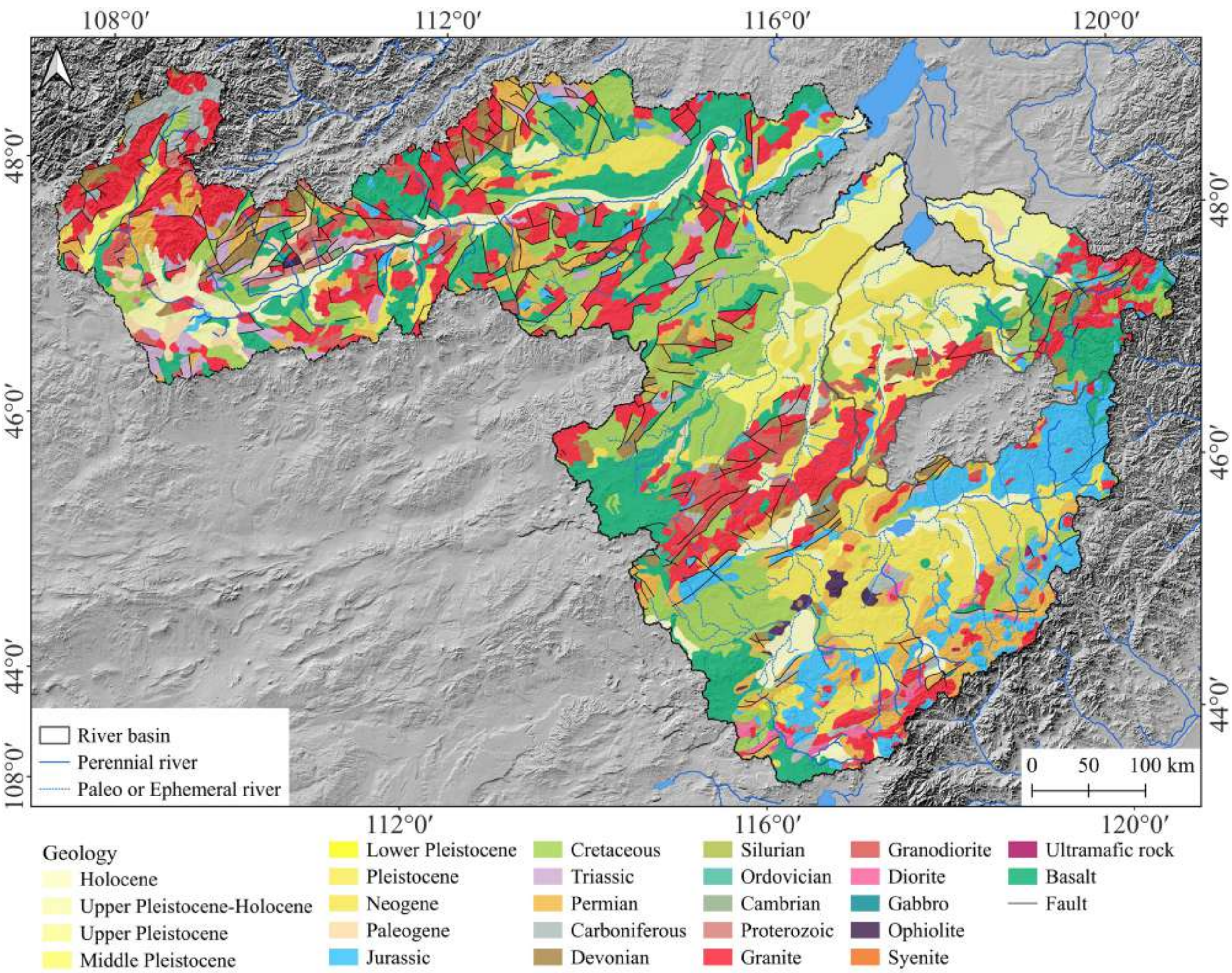

Fig. 2.Geological setting of the study area. Geological map compiled from Tomurtogoo et al. (1998) and Petrov et al. (2016), with fault data after Byamba (2012)

In addition, Quaternary depositional plains, comprising Neogene, alluvial, and lacustrine sediments, are also widely distributed across the region.

The Dariganga Volcanic Plateau occupies the southern part of the plain (Khukhuudei et al., 2024). This volcanic province covers approximately 10,000 km² and thickens southeastward, reaching a maximum thickness of 1,400 m (Gerel, 2012). Approximately 222 volcanic edifices have been identified in this region, and volcanic activity in the Dariganga Volcanic Plateau is interpreted to have commenced during the Middle Miocene (Vlodavets, 1950; Kepezhinskas, 1979; Gerel, 2012).

Building upon the regional landscape evolution described above, the present-day drainage systems represent a relict fluvial network that is no longer active, with no observable surface flow. However, the widespread occurrence of Middle Pleistocene and Upper Pleistocene-Holocene sedimentary deposits along these paleo valleys provides direct geological evidence that these rivers were actively flowing and perennial during these periods (Fig. 2).

The map highlights the distribution of Pleistocene to Holocene fluvial depositional units, Mesozoic-Cenozoic sedimentary and volcanic formations, and various Paleozoic rock units (including Permian, Carboniferous, and Devonian strata), thereby clearly illustrating their spatial arrangement across the study area.

Within the Wulagai River basin, the mean annual air temperature is -0.9°C, with annual precipitation ranging from 250 to 400 mm, whereas in the Xilin River basin, the mean annual air temperature is 1.7°C and annual precipitation is approximately 266 mm (Pang, 2011; Zhou et al., 2024).

The Greater Khingan Mountains represent a Mesozoic-Cenozoic orogenic belt developed upon earlier Caledonian and Hercynian (early and late phases) folded basement structures (Tomurtogoo, 2012). Volcanic activity in this region began during the Jurassic, resulting in the widespread distribution of intermediate to felsic volcanic rocks of Jurassic age, as well as Yanshanian intermediate to felsic intrusive bodies (Petrov et al., 2016; Deru et al., 2017). The basement is predominantly composed of Paleozoic-Mesozoic intrusive rocks.

DATA

This study utilizes multiple global-scale remote sensing and climatic datasets to characterize the geomorphology and environmental conditions of paleo-drainage basins in Eastern Mongolia. Paleo-drainage basins were identified based on a combination of geomorphological indicators, including longitudinal profile continuity, alignment of dry valleys, and spatial association with lacustrine depressions. These criteria were manually validated using satellite imagery. These criteria were manually validated using high-resolution satellite imagery (e.g., Google Earth Pro), focusing on valley continuity, channel morphology, and alignment of lacustrine depressions.

The SRTM DEM (30 m and 90 m resolution) was used as the primary topographic dataset to

Table 1. Data sources used in the study

Dataset	Source	Spatial resolution	Temporal coverage	Data access	Purpose of this study
SRTM DEM	USGS	30 m / 90 m	2000	Google Earth Engine	Basin delineation, slope, and relief analysis
MODIS NDVI (MOD13)	NASA MODIS	250-500 m	2000-present	Google Earth Engine	Vegetation cover analysis
MODIS LST (MOD11)	NASA MODIS	~1 km	2000-present	Google Earth Engine	Land surface temperature
MODIS ET (MOD16)	NASA MODIS	~500 m	2000-present	Google Earth Engine	Evapotranspiration estimation
WorldClim precipitation	WorldClim v2	~1 km	1970-2000	WorldClim database	Mean annual precipitation distribution

derive morphometric parameters such as slope and local relief (Farr et al., 2007). DEM-derived drainage networks are subject to uncertainties related to spatial resolution and preprocessing steps, particularly in low-relief terrains. The uncertainty in basin delineation and morphometric parameters is estimated at ±3-5%, mainly due to DEM resolution and flow-routing sensitivity.

To characterize the geomorphology and environmental conditions of paleo-drainage basins in Eastern Mongolia, this study integrates remote sensing data and global climate datasets.

In addition, remotely sensed and climate datasets-including precipitation, LST, ET, and NDVI -were used to compare environmental conditions between paleo and active drainage basins. All environmental variables were spatially aggregated to the basin scale, and consistent thresholds were applied for comparative analysis.

Precipitation data were obtained from the WorldClim v2 global climate database, representing interpolated meteorological observations for 1970-2000 at ~1 km spatial resolution (Fick and Hijmans, 2017). MODIS satellite products processed in Google Earth Engine (GEE) (Gorelick et al., 2017) were used to derive NDVI (MOD13; Didan et al., 2015), LST (MOD11; Wan et al., 2015), and ET (MOD16; Mu et al., 2011). These datasets provide continuous observations since 2000 and are widely applied in environmental and hydrological studies (Wan et al., 2015; Didan et al., 2015).

METHODS

Topographic analysis was conducted using SRTM DEMs at 30 m and 90 m spatial resolutions. Before analysis, the DEMs were preprocessed in QGIS. Spurious depressions were removed using the Fill Sinks tool to ensure hydrological consistency. Flow direction and flow accumulation were then derived using the D8 algorithm, enabling the extraction of a hydrologically consistent drainage network. Drainage basins were delineated based on DEM-derived hydrological parameters combined with geomorphological interpretation. Key morphometric variables, including slope and local relief, were calculated from the DEM.

To evaluate hydrological and ecological differences between paleo and active drainage basins, NDVI, LST, and ET were analyzed at the basin scale. NDVI reflects vegetation density and biological activity (Tucker, 1979; Huete et al., 2002), LST represents surface thermal conditions and aridity (Wan et al., 2015; Coll et al., 2005), and ET describes water flux dynamics within the hydrological cycle (Oki and Kanae, 2006; Jasechko et al., 2013).

Paleo-drainage identification criteria

Paleo-river channels were identified based on a combination of geomorphological and topographic criteria. These include (i) continuity of longitudinal profiles, (ii) downstream alignment of connected depressions, (iii) presence of linear valley-like features observable in DEM-derived hillshade and satellite imagery, and (iv) systematic spatial linkage of lacustrine basins suggesting overflow connections between adjacent depressions. Isolated closed depressions lacking downstream connectivity were excluded from the reconstruction.

Hypsometric Curve (HC)

The HC illustrates the relationship between area and elevation within a drainage basin (Eq. 1; Strahler, 1952; Schumm, 1956):

$$f_x = \{ f(y) \} \quad (1)$$

In this equation, x -corresponds to the normalized cumulative area (a/A) and y -denotes the normalized cumulative elevation (h/H), where:

- a -represents the surface area enclosed by a given contour,
- A -is the total area of the drainage basin,
- h -indicates the elevation within that contour, and
- H -is the maximum elevation of the basin.

Both axes are scaled from 0 to 1. The form of the curve reflects the degree of landscape dissection and provides insight into the basin's developmental stage (Strahler, 1952). In this study, hypsometric curves for four drainage basins were generated using QGIS.

Hypsometric Integral (HI)

The HI is a quantitative measure used to describe the elevation distribution within a drainage basin (Strahler, 1952). It corresponds to the area under the hypsometric curve and represents the proportion of the original landmass that remains uneroded (Keller and Pinter, 2002; Hassen et al., 2014).

$$HI = \frac{H_{mean} - H_{min}}{H_{max} - H_{min}} \quad (2)$$

where, H_{mean} -mean elevation, H_{min} -minimum elevation, H_{max} -maximum elevation

Higher HI values indicate less-eroded landscapes and may suggest tectonic influence on basin morphology. In contrast, lower HI values reflect more advanced stages of erosion and relatively stable tectonic conditions. HI values greater than 0.5 indicate a youthful stage of landscape development, whereas values lower than 0.4 suggest mature to old-stage geomorphic conditions.

Basin Shape Index (B_s)

The B_s is defined as the ratio of basin length (B_l) to basin width (B_w) (Cannon, 1976; Larson et al., 2020; Enkhbold et al., 2025a, b; Batzorig et al., 2025).

Drainage basins in tectonically active regions tend to exhibit elongated shapes aligned with the main river course (Larson et al., 2020; Makrari et al., 2022). In contrast, under conditions of reduced tectonic activity and prolonged erosion, basin shapes gradually evolve toward a more circular form (Kumar et al., 2022).

$$B_s = \frac{B_l}{B_w} \quad (3)$$

In this study, B_l -was measured from the basin outlet to the most distant point along the main drainage axis, whereas B_w -was defined as the basin's maximum width.

RESULTS

Reconstruction of Paleo-Hydrological Networks: Based on GIS-based geomorphological analysis and longitudinal profile continuity, two major paleo-hydrological systems were identified between the currently active Khalkh and Kherlen River basins in Eastern Mongolia. These reconstructed paleo-rivers originated from the Nukht Davaa and the Khingan Mountains, forming extensive drainage networks across the Eastern Mongolian Plain.

The first paleo-hydrological system was located adjacent to the Khalkh River basin. The reconstructed flow path extends through the valleys of the Azarga and Shine Rivers within Khalkhgol soum. It continues through a series of depressions, including Uvur Khooloi, Orokhyn Khooloi, Tamsagiin Khooloi, and Adag Doloonii Khooloi. The system then passes through Baruun, Dund and Zuun Shavar Lake before reaching the southwestern part of Buir Lake (Fig. 3).

The second paleo-hydrological system was situated along the boundary of the Kherlen River basin. This Paleo River originated from the headwaters of the Wulagai and Xilin Rivers on the western slope of the Khingan Range in present-day China. It flowed northwestward through Bichigtiin Zuun Khooloi, Targanii Tal, Khaltaryn Gobi, Erenii Eregtseg, and Uneet Eregtseg, reaching the vicinity of Baga Khuree. From there, it turned northeastward and joined the Orshuun River via Menengiin Tsagaan Khooloi and Muu Khudgiin Khooloi (Fig. 4).

Longitudinal profiles extracted along the reconstructed paleo-channels reveal well-defined valley morphology, characterized by broad, shallow, channelized depressions (Table 2; Fig.

Table 2. Morphometric parameters used in the study

№	Parameters	Khalkh River	Kherlen River	Paleo River 1	Paleo River 2
1	Area (km^2)	16584.7	98145.3	20706.6	140804.5
2	River length (km)	334	1156	261	896
3	Basin length (km)	241	729	214.3	562.9
4	Basin width (km)	151	276	194.2	470.7
5	Maximum elevation (m)	1740	2477	1198	1946
6	Mean elevation (m)	953	1124	775.9	980.3
7	Minimum elevation (m)	575	537	572	558
8	Hi	0.32	0.3	0.33	0.3
9	Bs	1.6	2.64	1.1	1.2
10	Basin relief (m)	1165	1940	626	1388
11	Basin slope (°)	4.62	3.28	1.36	2.27

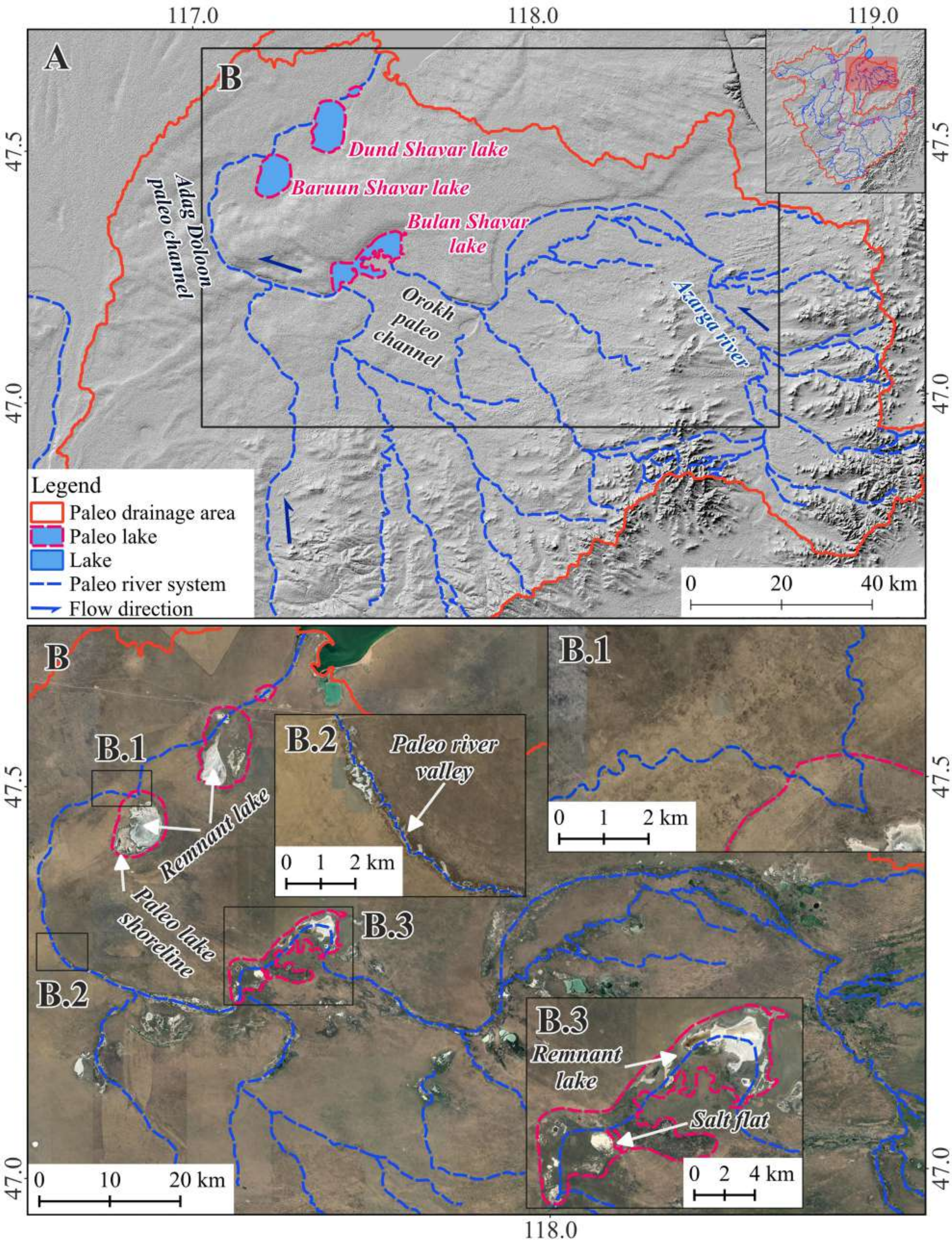

Fig. 3. Paleo Basin-1: Paleo-drainage and paleo-lake features**. (A)** Shaded relief maps showing the paleo-drainage areas (red outlines), paleo lakes (pink outlines), and reconstructed paleo-river systems (blue dashed lines with flow direction indicated by arrows). Arrows indicate inferred paleo-flow directions. **(B)** High-resolution satellite images of the boxed area in panel A show geomorphic features of paleo-lake shorelines, salt flats, and paleo-river valleys and channels. Insets (B.1, B.2, B.3) highlight detailed morphologies of paleo-lake remnants and fluvial systems

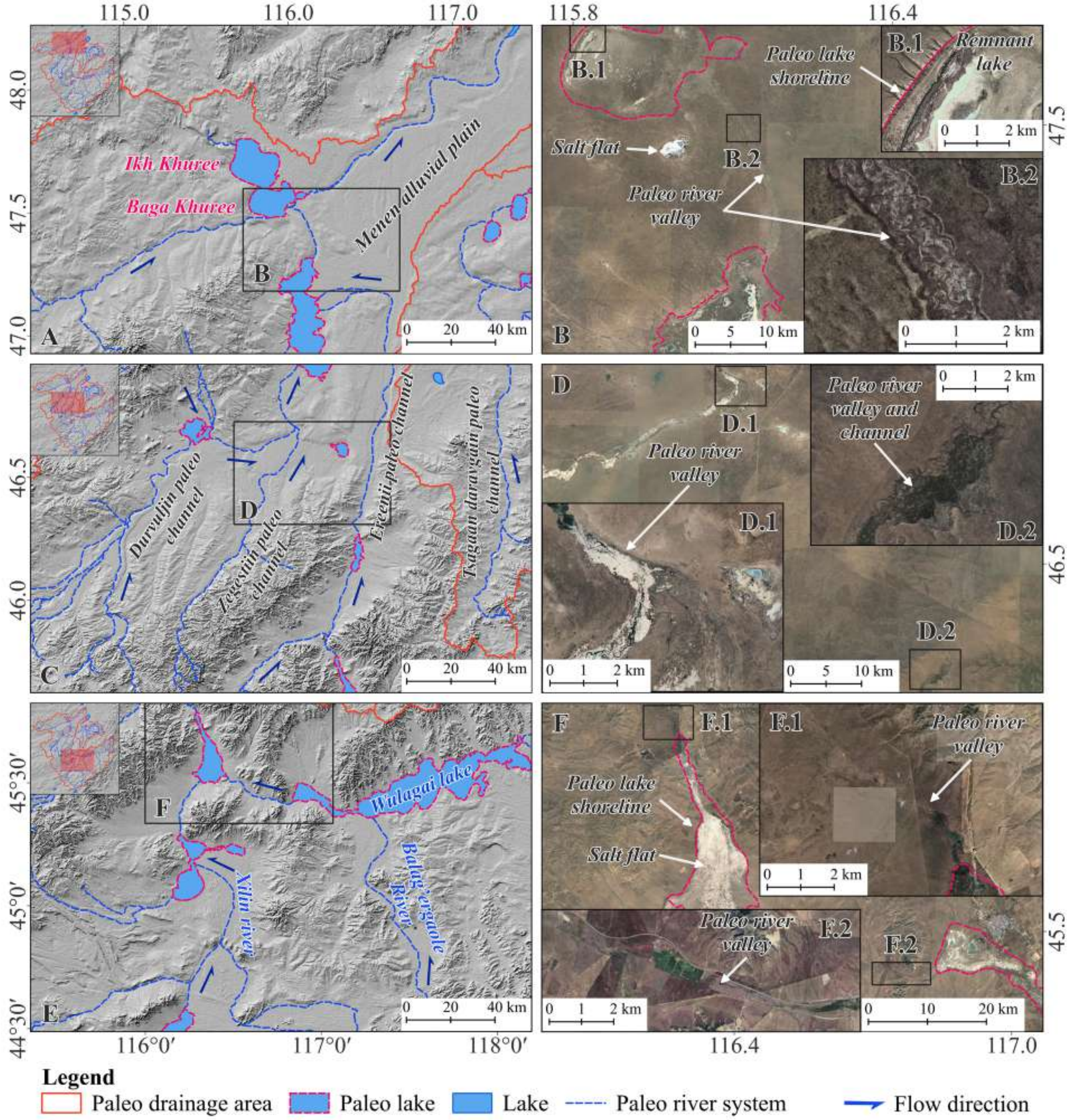

Fig. 4. Paleo Basin-2: Paleo-drainage and paleo-lake features. (A, C, E) Shaded relief maps showing the paleo-drainage areas (red outlines), paleo lakes (pink outlines), and reconstructed paleo-river systems (blue dashed lines with flow direction indicated by arrows) for three sub-regions of the basin. Arrows indicate inferred paleo-flow directions. (B, D, F) High-resolution satellite images of the boxed areas in panels A, C, and E, respectively, show geomorphic features of paleo-lake shorelines, salt flats, and paleo-river valleys and channels. Insets (B.1, B.2; D.1, D.2; F.1, F.2) highlight detailed morphologies of paleo-lake remnants and fluvial systems. B, B.1, B.2: Paleo-lake shoreline remnants and paleo-river valleys near Ikh Khuree and Baga Khuree. D, D.1, D.2: Paleo-river valleys and channels along the Ereeniin paleo channel and adjacent systems. F, F.1, F.2: Paleo-lake shorelines, salt flats, and paleo-river valleys near Wulagai Lake and the surrounding drainage system

5). Compared with modern active river systems, the paleo-rivers exhibit lower relief and gentler longitudinal gradients, suggesting reduced fluvial energy and discharge capacity.

These morphometric characteristics indicate that hydraulic gradients were likely insufficient to sustain persistent channelized flow under the present climatic regime. In low-relief environments, reduced slope gradients lead to lower flow velocities and enhanced water loss through infiltration and evaporation, thereby limiting effective runoff generation (Pike et al., 2009; Evans, 2012).

Importantly, the spatial arrangement of these valleys suggests that the paleo-drainage systems functioned as a series of interconnected lacustrine

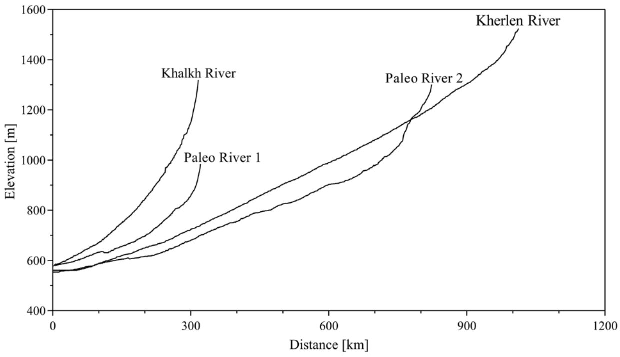

Fig. 5. Longitudinal profiles along the rivers of paleo and active drainage basins

and fluvial depressions, where overflow between adjacent basins contributed to downstream connectivity along reconstructed flow paths (Fig. 6).

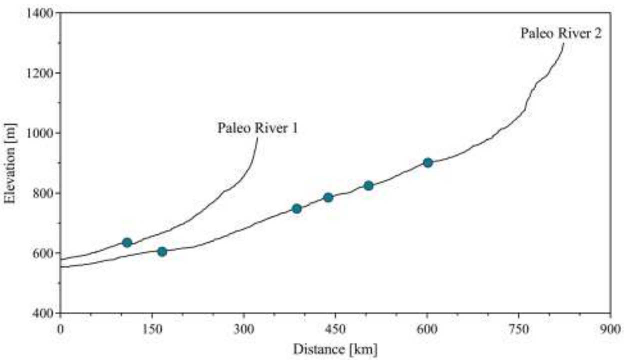

Fig. 6. Longitudinal profiles along paleo-rivers and the location of lakes. Green dots indicate lakes located along river valleys

Morphometric Characteristics of the Basins: Morphometric analysis of SRTM data indicates that Paleo River 1 had an area of 20,706.6 km² and a length of 261 km. In contrast, Paleo River 2 was considerably larger, with an area of 140,804.5 km² and a length of 896 km. Both systems were northward flowing with gentle gradients (2.39 and 1.55 m/km, respectively), comparable to those of the present-day Khalkh and Kherlen Rivers.

The widths of paleo-valleys exceed 10 km in some sections. These paleo-basins extended across both Mongolia and China, collecting runoff from the Khingan Range, Nukht Davaa, the Dariganga Volcanic Plateau, and the Middle Khalkh uplands. Paleo Basin 1 consists of two main sub-basins sourced from elevated terrains to the west and southeast, whereas Paleo Basin 2 comprises four major sub-basins originating from similar elevated terrains.

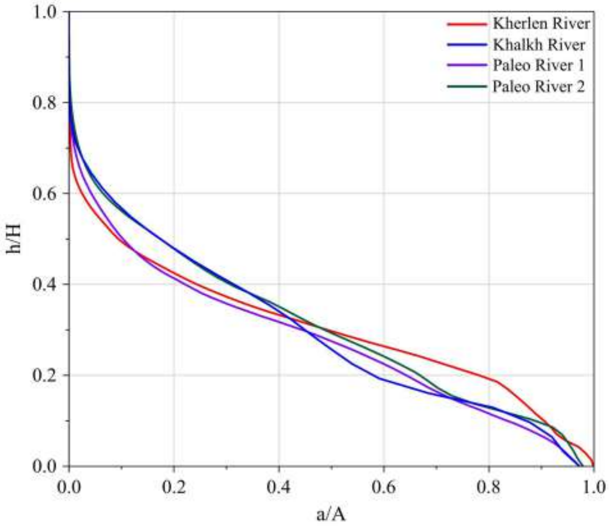

Fig. 7. Hypsometric curves of paleo and active drainage basins

The HI values range between 0.30 and 0.33, indicating that these basins are at comparable stages of geomorphic development (Fig. 7). Total relief varies from 626 m (Paleo River 1) to 1940 m (Kherlen River basin) (Table 2). These values suggest that both paleo and active basins are at comparable stages of geomorphic evolution, indicating that differences in hydrological behavior are more likely driven by climatic and topographic factors than by tectonic stage.

The *Bs* show a clear distinction between active and paleo basins. Active drainage basins are more elongated (*Bs* = 1.6-2.64), whereas paleo basins exhibit more rounded forms (*Bs* = 1.1-1.2), reflecting differences in basin geometry and drainage organization.

The relatively low basin shape index (*Bs*) values of paleo-basins indicate a tendency toward more circular geometries, which are commonly associated with reduced tectonic forcing and prolonged geomorphic stabilization. This suggests that tectonic activity may have played a secondary role compared to climatic controls in shaping the paleo-drainage systems.

Topographic Characteristics: The spatial distribution of local relief and slope reveals clear contrasts within the study area. The highest values are observed in the mountainous regions of the Khentii and Greater Khingan Mountains, whereas the Eastern Mongolian Plain shows relatively low values (Figs. 8-10).

The cross-sections indicate that paleo-river

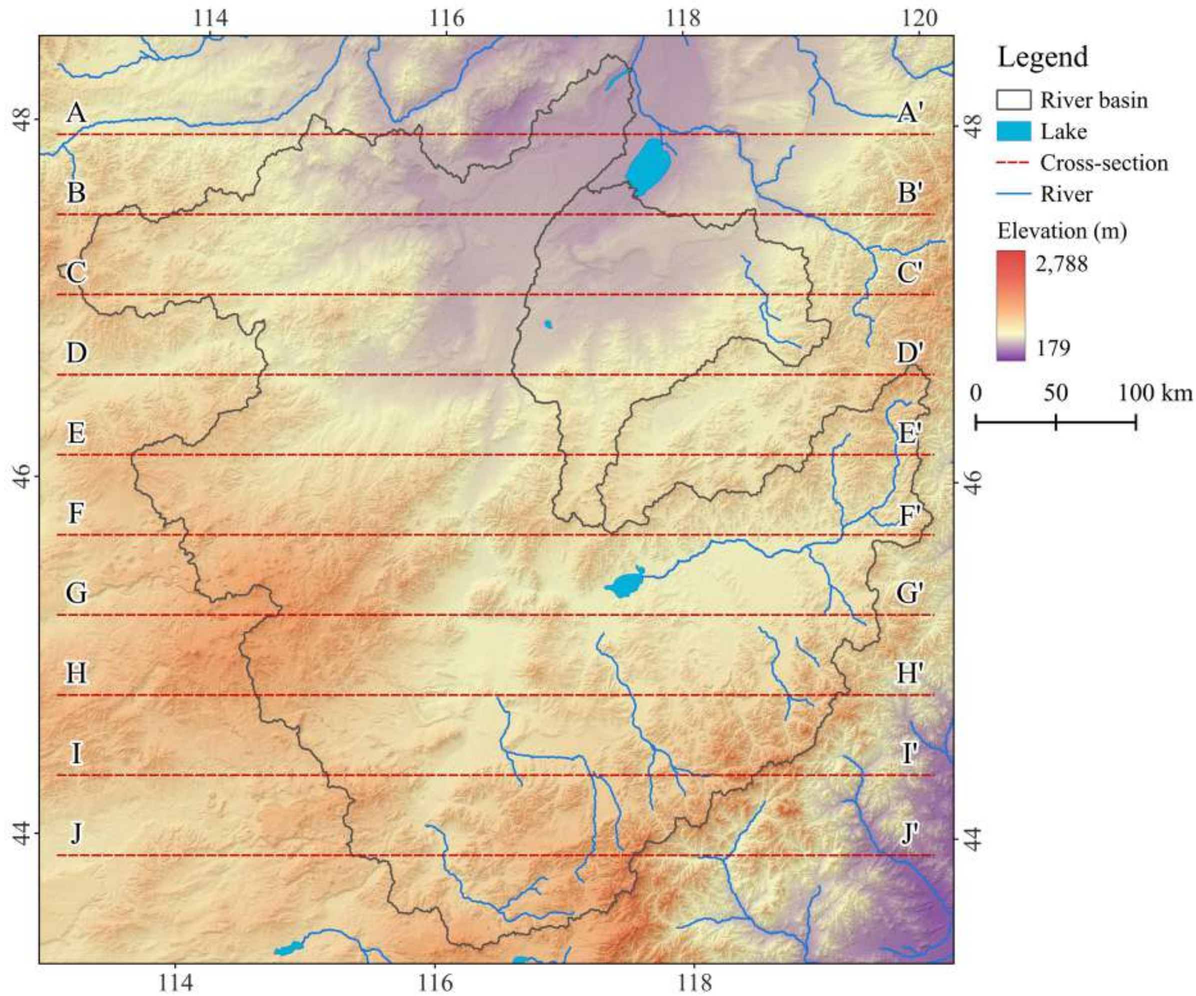

Fig. 8. Locations of cross-sections performed across the paleo-basins

valleys are generally wide and shallow, with relatively gentle and uniform slopes (Fig. 9). This suggests that they formed under conditions of low flow energy and prolonged erosion. Such morphology reflects a geomorphologically stable environment, where strong tectonic uplift was not the dominant controlling factor.

The A-J transect shows a clear spatial variation in relief from west to east. In the A-D segment, the terrain is low and smooth, dominated by broad and shallow paleo-valleys, indicating relatively stable surface conditions. In the E-G segment, the relief gradually increases, and the influence of the Dariganga Volcanic Plateau becomes apparent, leading to slight changes in valley morphology. Toward the J segment, the transect approaches the Greater Khingan Mountains, where elevation differences and slope gradients increase significantly, and variations in surface morphology become more pronounced (Fig. 9).

The comparative analysis of local relief, slope gradient, and mean annual precipitation across the four river systems reveals distinct differences between active and paleo-river basins (Fig. 11).

In terms of local relief (Fig. 11A), both active river systems (Khalkh and Kherlen) show a relatively broader distribution across low to moderate relief classes. In contrast, paleo-river systems are strongly concentrated in the lowest relief classes (~100-200 m). In particular, Paleo River 1 exhibits a pronounced peak in the lowest relief category, indicating highly restricted low-relief geomorphic conditions, while Paleo River 2 shows a slightly broader but still low-relief-dominated distribution.

Slope gradient patterns (Fig. 11B) further highlight this contrast. Active river basins are characterized by a wider range of slope values, including a noticeable proportion of moderate slopes (5-15°), reflecting more diverse topographic settings. In contrast, both paleo-river systems are strongly concentrated in very gentle

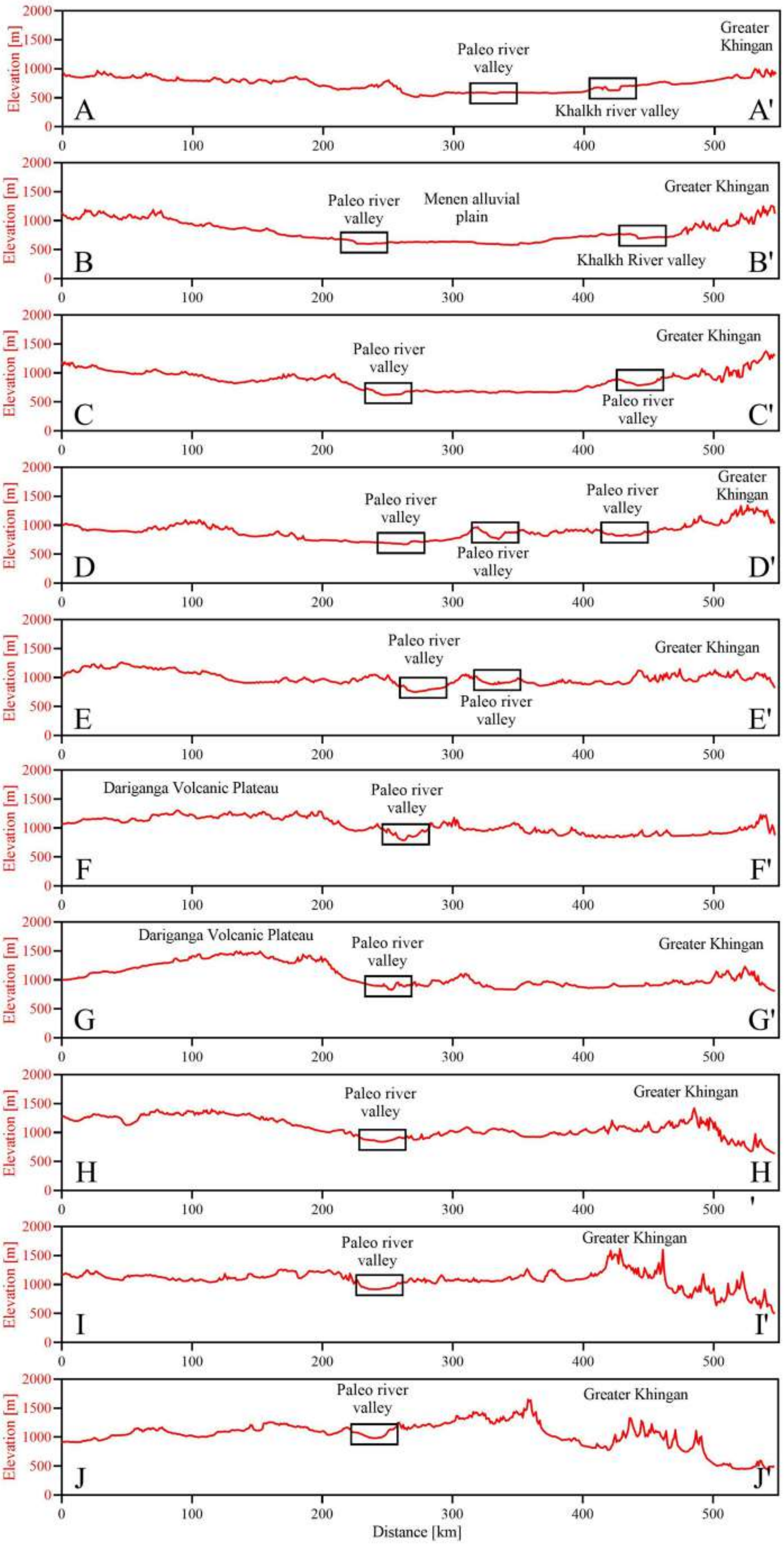

Fig. 9. Surface cross-sections were carried out in paleo-basins

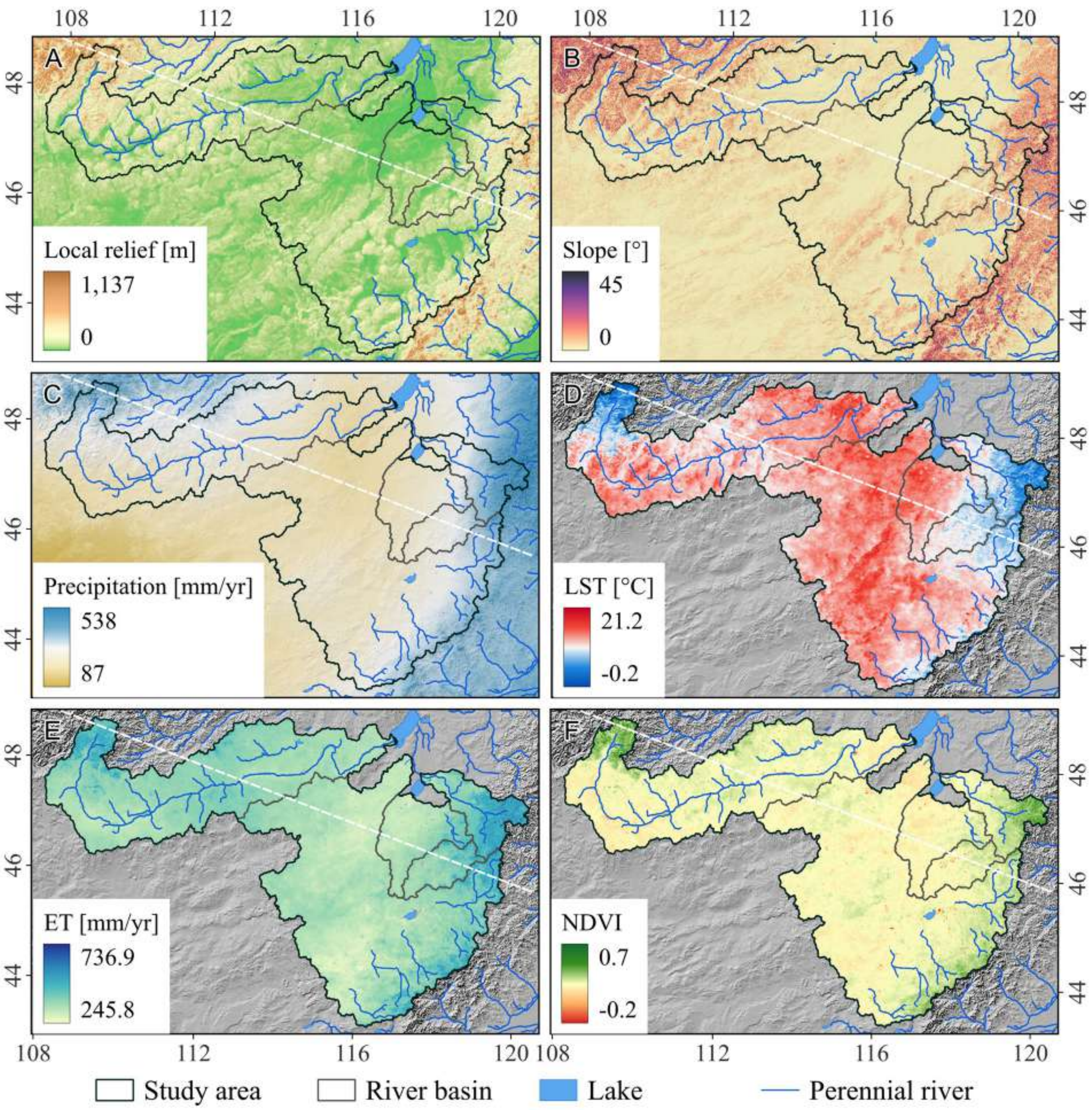

Fig. 10. Spatial distribution of local relief, slope, precipitation, LST, ET, and NDVI across the study area

slope values (<5°), with minimal representation in higher gradient categories, indicating highly subdued and uniform terrain conditions.

For mean annual precipitation (Fig. 11C), all river systems fall within broadly comparable climatic ranges; however, active rivers show a slightly wider distribution toward higher precipitation classes (~300-500 mm/yr). Paleo-river systems, particularly Paleo River 1, are more concentrated within intermediate precipitation ranges, with reduced variability compared to active basins.

Overall, the results demonstrate that paleo-river systems are consistently associated with lower relief, gentler slopes, and more restricted environmental variability compared to active river systems, while precipitation differences remain relatively minor and overlapping (Table 3).

Climatic and Vegetation Indicators: The spatial distributions of precipitation, ET, NDVI, and LST exhibit distinct patterns across the study area (Figs. 10 and 12).

Precipitation is relatively high in the mountainous regions of the Khentii and Greater Khingan Mountains and decreases toward the Eastern Mongolian Plain. In paleo-basins, areas receiving less than 250 mm of annual precipitation account

Table 2. Descriptive statistics of local relief, slope gradient, and mean annual precipitation for two active river systems (Khalkh and Kherlen) and two paleo-river systems (Paleo River 1 and Paleo River 2). Values are presented as mean ± standard deviation and minimum-maximum ranges

River / Basin	Local relief (m) Mean ± SD	Local relief (m) Min-Max	Slope (°) Mean ± SD	Slope (°) Min-Max	Precipitation (mm/yr) Mean ± SD	Precipitation (mm/yr) Min-Max
Khalkh	165.65 ± 118.25	0-658	4.62 ± 4.90	0-40.69	370.30 ± 66.90	242-516
Kherlen	143.04 ± 105.53	0-881	3.28 ± 3.71	0-45.23	268.85 ± 44.25	187-486
Paleo River 1	58.04 ± 40.71	0-307	1.36 ± 1.37	0-23.20	257.20 ± 31.13	208-374
Paleo River 2	95.95 ± 67.32	0-681	2.27 ± 2.50	0-36.84	262.79 ± 52.82	185-449

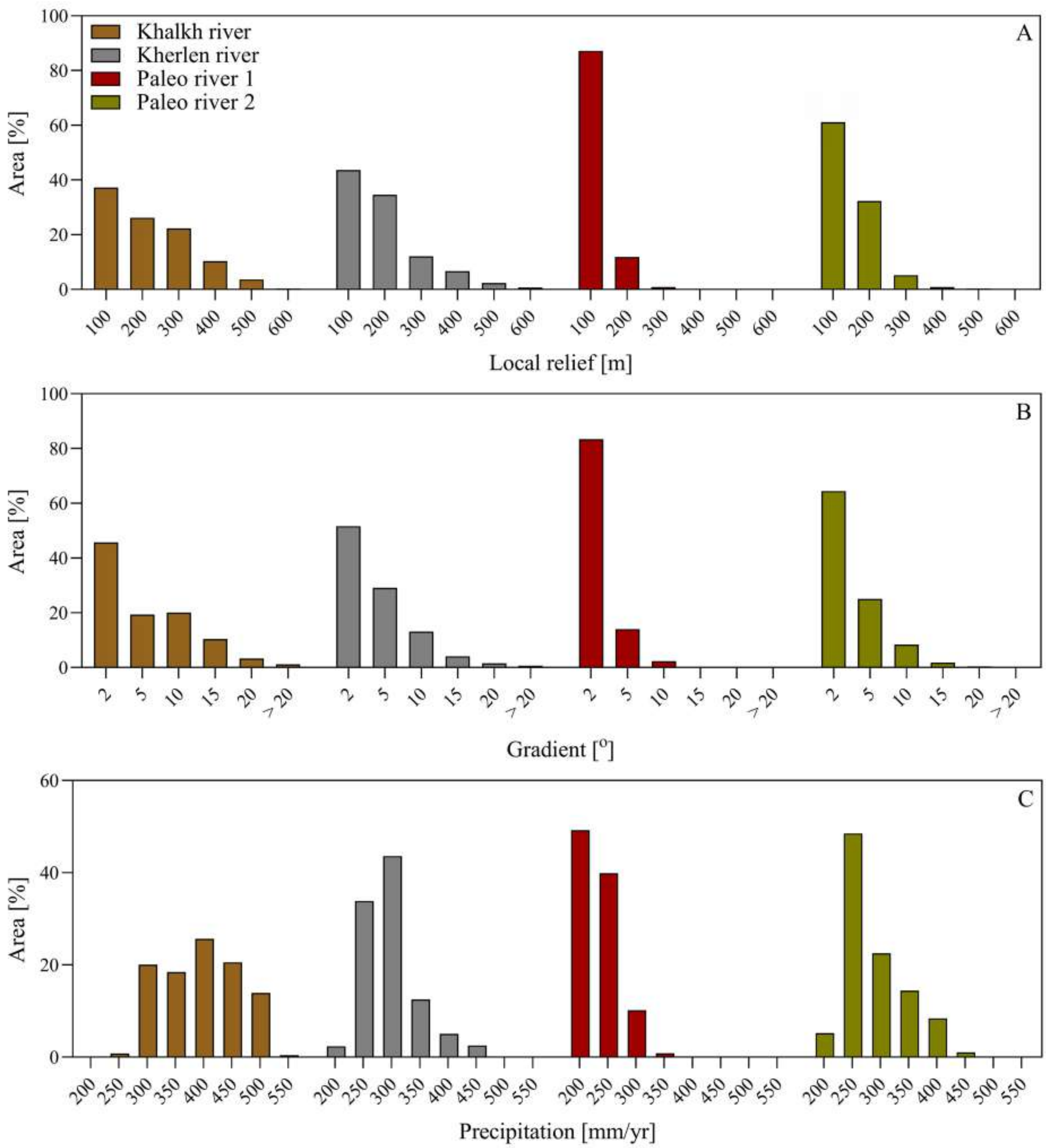

Fig. 11. Percentage area of local relief, slope, and precipitation for each river basin. Note: Values on the X-axis represent the percentage of basin area (%) corresponding to each relief, slope, and precipitation class

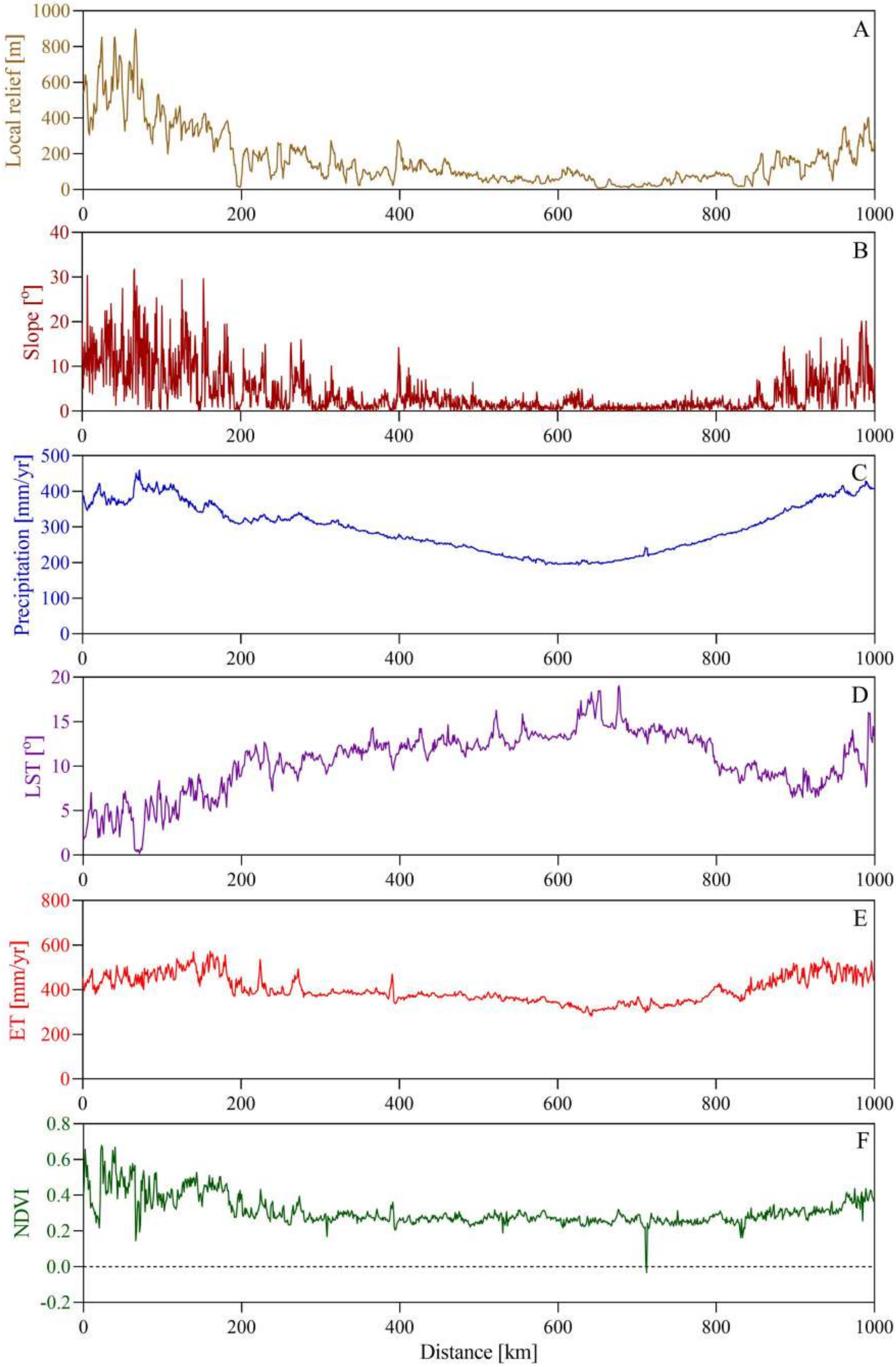

Fig. 12. Variations of indices along transects used in the study. Eastern Mongolia exhibits lower relief, precipitation, evapotranspiration, and vegetation index values than the Khentii and Greater Khingan Mountains and nearby highlands

for more than half of the total basin area, whereas this proportion is less than 40% in active basins. These observations indicate that precipitation thresholds exert a primary control on hydrological connectivity. In semi-arid regions, annual precipitation below approximately 250 mm is generally insufficient to maintain perennial flow, particularly in low-gradient basins where evapotranspiration losses are high (Fig. 11).

NDVI values are higher in mountainous regions, indicating denser vegetation, while lower values predominate in the plains. ET shows a similar spatial pattern, with higher values in active river basins than in paleo-basins.

LST exhibits an inverse relationship with elevation and vegetation cover, with lower values in mountainous areas and higher values in lowland plains. Paleo-basins generally show higher LST values than active basins.

Previous studies have demonstrated that topographic, climatic, and biophysical factors-such as relief, slope, precipitation, evapotranspiration, and vegetation cover-play a critical role in controlling surface runoff and water yield (Feng et al., 2023; Gan et al., 2021; Liu et al., 2018). The spatial patterns observed in this study suggest that these factors significantly influence the hydrological characteristics of the investigated basins (Figs. 11-12).

DISCUSSION

This study presents the first reconstruction of paleo-drainage basins in Eastern Mongolia using GIS-based geomorphological analysis. The results indicate that paleo-basins differ markedly from currently active basins in terms of morphometry, topography, and environmental conditions (local relief, slope, precipitation, ET, NDVI, and LST).

Specifically, more than 90% of paleo-basin areas exhibit slopes below 5° and local relief below 200 m, suggesting low-energy, unstable flow conditions with limited water accumulation. Contemporary climatic conditions, characterized by low precipitation, sparse vegetation (NDVI), and relatively high LST, further indicate that these regions are currently dominated by arid and warm environments that are unfavorable for sustaining stable surface flow.

Activity and Hydrological Evolution of Paleo-Basins:

Although both paleo and active drainage basins fall within a similar stage of landscape development (HI = 0.30-0.32), the paleo-basins are predominantly located in low-relief terrains, where more than 90% of their area is characterized by relative relief below 200 m. Furthermore, regions receiving less than 250 mm of annual precipitation occupy the majority of the paleo-basin area, indicating a limited water supply.

In contrast, the active Khalkh and Kherlen River basins are situated in regions with steeper slopes, higher local relief, and greater precipitation (>250-300 mm), providing more favorable hydrological conditions for sustaining perennial flow. These morphometric differences likely reflect weaker hydrological activity in paleo-basins, associated with less favorable environmental conditions for maintaining stable runoff.

GIS-based reconstruction, supported by satellite imagery and cross-sectional analyses, indicates that the paleo-rivers were connected through a series of lakes. Excess water from one lake likely overflowed into adjacent basins, forming a continuous hydrological network. The spatial alignment of lacustrine depressions along reconstructed flow paths, together with the continuity of longitudinal profiles, supports the interpretation that these features represent remnants of integrated paleo-drainage systems rather than isolated geomorphic depressions.

Importantly, geomorphological evidence from Eastern Mongolia further supports the existence of former fluvial systems. Murzaev (1952) documented well-preserved fluvial terraces and ancient dry channels across the Menen and Buir Lake plains, indicating the presence of extensive paleo-drainage networks in the region. These terraces are situated approximately 1.5 m and 3.5-4.0 m above valley floors and are spatially associated with broad valley systems and lacustrine depositional surfaces.

Previous studies in northern, western, and southern Mongolia (e.g., the Khuvsgul, Darkhad Depression, Great Lakes Depression, and Valley of Lakes) have demonstrated that glacial processes played a significant role in increasing lake levels (Grunert et al., 2000; Tarasov et al., 2000; Lehmkuhl and Lang, 2001; Klinge et al., 2021; Enkhbold et al., 2026). In contrast, paleo-hydrological changes in Eastern Mongolia were more likely controlled by climatic factors, particularly fluctuations in the summer monsoon and increasing aridity (Harrison et al., 1996).

Paleoclimatic Context

This interpretation is supported by regional paleoclimate evidence. Palynological studies from Wulagai Lake indicate that during the mid-late MIS 3 period (~43,800-29,500 cal BP), humid conditions prevailed, with steppe vegetation dominating and relatively high lake levels. During MIS 2 (29,500-10,600 cal BP), increasing aridity led to a reduction in lake size, while the Holocene (MIS 1; 10,600 cal BP to present) has been characterized by generally semi-arid conditions (Li et al., 2019) (Fig. 13).

The humid conditions during MIS 3 likely supported interconnected lake systems and continuous drainage connectivity across Eastern Mongolia. Subsequent increases in solar insolation and reductions in glacial extent enhanced evaporation rates, contributing to a progressively negative regional water balance (Shi et al., 1999, 2001; Berger and Loutre, 1991; de Boer et al., 2014). Under these conditions, the relatively flat and low-precipitation paleo-basins of Eastern Mongolia would have been particularly sensitive to reductions in water input, ultimately leading to flow discontinuities and drainage fragmentation. Hydrological evolution during the Holocene appears to have been non-uniform. Residual fluvial activity may have persisted during the Early Holocene under relatively favorable moisture conditions, as suggested by geomorphic evidence including terrace formation and paleochannel preservation (Murzaev, 1952).

Climate-Topography Controls on Hydrological Connectivity

The evolution of paleo-drainage systems in Eastern Mongolia can be conceptualized as a coupled climate-topography system. During humid intervals (MIS 3), increased precipitation and reduced evapotranspiration likely resulted in positive water balance conditions, enabling the development of interconnected lake systems and continuous fluvial connectivity (Herzschuh, 2006; An et al., 2008).

As climatic conditions shifted toward aridity during MIS 2 and the Holocene, decreasing precipitation and increasing evapotranspiration led to progressively negative water balance conditions (Feng et al., 2023; Gan et al., 2021). In low-relief basins, this transition promoted hydrological disconnection, fragmentation of lake systems, and eventual cessation of surface flow. Similar hydrological sensitivity to climatic thresholds has been widely documented across

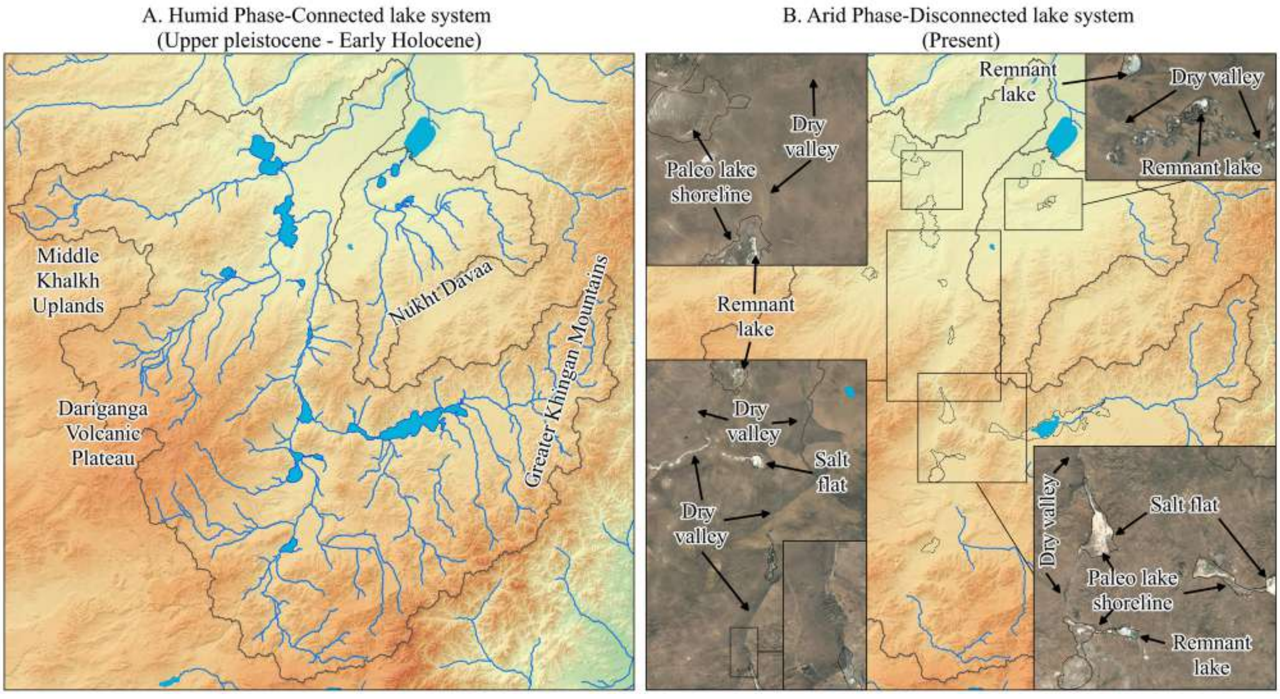

Fig. 13. Evolution of a Former Interconnected Lake System in Eastern Mongolia and Northeastern China

semi-arid regions of Central Asia (Herzschuh, 2006; Liu et al., 2018).

Comparable hydrological transitions have also been reported from the Mongolian Altai and Tien Shan regions, where relatively small climatic shifts produced substantial changes in lake levels and drainage connectivity (Herzschuh, 2006; Liu et al., 2018; Klinge et al., 2021). Similar threshold behavior has been documented in these regions, where minor climatic fluctuations resulted in significant shifts in lake levels and drainage integration (Hagg et al., 2007; Sorg et al., 2012; Bolch et al., 2019).

These observations suggest that hydrological systems in semi-arid continental interiors may exhibit strongly non-linear responses to climatic forcing, particularly near critical precipitation thresholds. Small changes in precipitation or evapotranspiration can trigger disproportionate shifts between connected and fragmented drainage states. Such threshold-driven behavior is especially pronounced in low-relief terrains, where limited hydraulic gradients further constrain runoff generation and flow persistence.

In addition, topographic constraints such as low slope gradients and reduced relief further limit runoff generation and flow persistence, reinforcing the importance of geomorphological controls on hydrological evolution (Evans, 2012; Pike et al., 2009).

Overall, the results suggest that paleo-drainage evolution in Eastern Mongolia was governed by the interaction between climatic forcing and topographic constraints. This threshold -controlled behavior highlights the sensitivity of semi-arid hydrological systems to relatively small climatic changes and provides a useful framework for interpreting paleo-hydrological disconnection processes across dryland environments. The conceptual model may also apply to other semi-arid continental interiors where hydrological connectivity is controlled by climatic thresholds.

CONCLUSIONS

This study reconstructed paleo-drainage basins in Eastern Mongolia using GIS-based geomorphological methods and compared their morphometric and environmental characteristics with those of present-day active river basins.

The main conclusions are summarized as follows:

First, previously unrecognized paleo-drainage basins were identified through DEM-based geomorphological analysis and mapping. The results suggest that these basins were once part of an interconnected hydrological system linked by multiple lakes, indicating that the hydrological network of Eastern Mongolia was more extensive in the past than it is today.

Second, morphometric analysis shows that paleo-basins are characterized by lower slopes, reduced local relief, and more planar surfaces compared to the active Khalkh and Kherlen River basins. These characteristics likely reflect weaker hydrological conditions and limited capacity for sustaining stable runoff.

Third, environmental variables-including precipitation, NDVI, LST, and ET-show clear spatial differences between paleo and active basins. Paleo-basins are predominantly located in low-precipitation, low-relief regions, which likely constrained the long-term persistence of surface flow.

Fourth, comparison with regional paleoclimate studies indicates that more humid conditions during the mid-late MIS 3 period likely supported more active hydrological systems. However, increasing aridity from MIS 2 onward, followed by semi-arid conditions during the Holocene, led to reduced water availability and the gradual weakening and eventual cessation of flow in paleo-basins.

Overall, this study demonstrates that the coupled effects of topographic constraints and climate-driven hydrological thresholds govern paleo-drainage evolution in semi-arid Eastern Mongolia. The results highlight the importance of non-linear system responses, where relatively small climatic variations can lead to substantial shifts in hydrological connectivity.

These findings suggest that threshold-controlled hydrological connectivity represents a fundamental characteristic of semi-arid continental basins, extending beyond the Mongolian context.

ACKNOWLEDGEMENTS

This study was carried out under the basic research project “Geomorphological New Subdivisions of Lake Districts in Mongolia,” supported by the Mongolian Foundation for Science and Technology and implemented during 2024-2026.

Authorship

Batzorig Batbold of conceptualization, methodology, software, formal analysis, writing, and editing, original draft preparation. Ulambadrakh Khukhuudei, Altanbold Enkhbold of conceptualization, investigation, writing, reviewing, and editing.

Complicit of interest

The authors declare that they have no conflict of interest. AI was used only for English grammar checking; all content, data, and interpretations are solely the authors' work.

REFERENCES

Altanbold, E., Ulambadrakh, Kh. 2022. Morphology and Origin of Lakes Depression in Mongolia. NUM Press Publishing, p. 188 (in Mongolian)

An, C-B., Chen, F-H., Barton, L. 2008. Holocene environmental changes in Mongolia: A review. Global and Planetary Change, vol. 63(4), p. 283-289. https://doi.org/10.1016/j.gloplacha.2008.03.007

Arzhannikova, A.V., Demonterova, E.I., Jolivet, M., Arzhannikov, S.G., Mikheeva, E.A., Ivanov, A.V., Khubanov, V.B., Pavlova, L.A., 2020. Late Mesozoic topographic evolution of western Transbaikalia: evidence for rapid geodynamic changes from the Mongol-Okhotsk collision to widespread rifting. Geoscience Frontiers, vol. 11(5). p. 1695-1709. https://doi.org/10.1016/j.gsf.2019.12.012

Batzorig, B., Ulambadrakh, K., Saruulzaya, A., Altanbold, E. 2025. Morphometric Analysis of the Numrug River Basin in Eastern Mongolia. Geographical Issues, vol. 25(02), p. 138-155 (in Mongolian with an English abstract). https://doi.org/10.22353/gi.2025.25.17

Bayanjargal, B., Nyamkhuu, M. 2017. Methodological issues in developing medium-scale geomorphological maps. Proceedings of the Mongolian Academy of Sciences, vol. 57(221), p. 82–92 (in Mongolian). https://doi.org/10.5564/pmas.v57i221.755

Berger, A., Loutre, M.F. 1991. Insolation values for the climate of the last 10 million years. Quaternary Science Reviews, vol. 10(4), p. 297-317. https://doi.org/10.1016/0277-3791(91)90033-Q

Bolch, T., Shea, J.M., Liu, S., Azam, F.M., Gao, Y., Gruber, S., Immerzeel, W.W., Kulkarni, A., Li, H., Tahir, A.A., Zang, G, Zhang, Y. 2019. Status and change of the cryosphere in the extended Hindu Kush Himalaya region. In The Hindu Kush Himalaya assessment: Mountains, Climate Change, Sustainability and People, p. 209-255. https://doi.org/10.1007/978-3-319-92288-1_7

Bridge, J.S. 2003. Rivers and Floodplains: Forms, Processes, and Sedimentary Records. Blackwell Science.

Byamba, J. 2012. Lithospheric Plate Tectonics. Byamba, J. (Ed.) Geology and Mineral Resources of Mongolia, Vol. III. Ulaanbaatar: Soyombo Printing. (in Mongolian)

Cannon, P.J. 1976. Generation of Explicit Parameters for a Quantitative Geomorphic Study of Mill Creek Drainage Basin. Oklahoma Geology Notes, vol. 36 (1), p. 3-16.

Chen, F., Yu, Z., Yang, M., Ito, E., Wang, S., Madsen, D.B., Huang, X., Zhao, Y., Sato, T., Birks, H.J.B., Boomer, I., Chen, J., An, C., Wünnemann, B. 2008. Holocene moisture evolution in arid central Asia and its out-of-phase relationship with Asian monsoon history. Quaternary Science Reviews, vol. 27(3-4), p. 351-364. https://doi.org/10.1016/j.quascirev.2007.10.017

Coll, C., Caselles, V., Galve, J.M., Valor, E., Niclos, R., Sánchez, J.M., Rivas, R. 2005. Ground measurements for the validation of land surface temperatures derived from AATSR and MODIS data. Remote sensing of Environment, vol. 97(3), p. 288-300. https://doi.org/10.1016/j.rse.2005.05.007

de Boer, B., Lourens, L.J., van de Wal, R.S. 2014. Persistent 400,000-year variability of Antarctic ice volume and the carbon cycle is revealed throughout the Plio-Pleistocene. Nature Communications., vol. 5, 2999._ __https://doi.org/10.1038/ncomms3999

Deru, X., Guoxiang, C., Yanhua, Z., Zhaochong, Z., Weidong, S. 2017. Yanshanian (Late Mesozoic) ore deposits in China - An introduction to the Special Issue. Ore Geology Reviews, vol. 88, p. 481-490.

https://doi.org/10.1016/j.oregeorev.2017.04.022
Didan, K., Munoz, A.B., Solano, R., Huete, A. 2015. MOD13Q1 MODIS/Terra Vegetation Indices 16-Day L3 Global 250m SIN Grid V006. NASA EOSDIS Land Processes DAAC. https://doi.org/10.5067/MODIS/MOD13Q1.006
Ding, Z., Lu, R., Wang, L., Yu, L., Liu, X., Liu, Y., Liu, L., Bai, M., Wang, S. 2021. Early-Mid Holocene climatic changes inferred from colors of eolian deposits in the Mu Us Desert. Geoderma, vol. 401, 115172. https://doi.org/10.1016/j.geoderma.2021.115172
Dorjsuren, B., Zemtsov, V.A., Batsaikhan, N., Demberel, O., Yan, D., Hongfei, Z.Yadamjav, O., Chonokhuu, S., Enkhbold, A., Ganzorig, B., Bavuu, E., Namsrai, O., Xiang, L., Yingjie, Y., Siyu, W. 2024. Trend analysis of hydro-climatic variables in the Great Lakes Depression region of Mongolia. Journal of Water & Climate Change, vol. 15(3), p. 940-957. https://doi.org/10.2166/wcc.2024.379
Enkhbold, A. 2021. Morphological classification and origin of lake depressions in Mongolia. Proceedings of the Mongolian Academy of Sciences, vol. 61(02), p. 35-43. https://doi.org/10.5564/pmas.v61i02.1758
Enkhbold, A., Khukhuudei, U., Seong, Y.B., Badarch, D., Tsedevdorj, S. O., Batbold, B., Ganbold, B. 2025b. Impact of faulting on the depression morphology of Ulaagchinii Khar Lake in Mongolia. Mongolian Geoscientist, vol. 30(61), p. 14-32. https://doi.org/10.5564/mgs.v30i61.3855
Enkhbold, A., Khukhuudei, U., Seong, Y.B., Dorligjav, S., Ganbat, S., Dorjsuren, B. 2026. Advances in lake-based limnological methods and research trends in Mongolia since 1990. Journal of Paleolimnology, vol. 74(3), 9. https://doi.org/10.1007/s10933-026-00389-z
Enkhbold, A., Khukhuudei, U., Seong, Y.B., Yadamsuren, G., Batbold, B., Davaasuren, D., Ganbat, Sh., Tsedevdorj, S., Bold, B., Badarch, D., Ganbold, B. 2025a. Tectonic geomorphology of the lake depressions in the Mongolian Altai mountains, western Mongolia. Frontiers in Earth Science, vol. 13, 1605844. https://doi.org/10.3389/feart.2025.1605844
Evans, I. S. 2012. Geomorphometry and landform mapping: What is a landform? Geomorphology, vol. 137(1), p. 94-106. https://doi.org/10.1016/j.geomorph.2010.09.029
Farr, T.G., Rosen, P.A., Caro, E., Crippen, R., Duren, R., Hensley, S., Kobrick, M., Paller, M., Rodriguez, E., Roth, L., Seal, D., Shaffer, S., Shimada, J., Umland, J., Werner, M., Oskin, M., Burbank, D., Alsdorf, D. 2007. The Shuttle Radar Topography Mission. Reviews of Geophysics, vol. 45(2). https://doi.org/10.1029/2005RG000183
Feng, P., Alifujiang, Y., Abuduwaili, J., Lu, N., Jiang, Y. 2023. Quantifying the impact of climate and vegetation changes on runoff based on the Budyko framework in the Lake Issyk-Kul Basin, Kyrgyzstan. Frontiers in Earth Science, vol. 11, 1251759. https://doi.org/10.3389/feart.2023.1251759
Fick, S.E., Hijmans, R.J. 2017. WorldClim 2: New 1-km spatial resolution climate surfaces for global land areas. International Journal of Climatology, vol. 37(12), p. 4302-4315. https://doi.org/10.1002/joc.5086
Florensov, N.A. 1978. Essays on structural geomorphology. Nauka, Moscow (in Russian)
Gan, G., Liu, Y., Sun, G. 2021. Understanding interactions among climate, water, and vegetation with the Budyko framework. Earth-Science Reviews, vol. 212, 103451. https://doi.org/10.1016/j.earscirev.2020.103451
Gerel, O. 2012. Intrusive Rocks. Byamba, J. (Ed.) Geology and Mineral Resources of Mongolia, vol. III. Ulaanbaatar, Soyombo Printing (in Mongolian)
Gorelick, N., Hancher, M., Dixon, M., Ilyushchenko, S., Thau, D., Moore, R. 2017. Google Earth Engine: Planetary-scale geospatial analysis for everyone. Remote Sensing of Environment, vol. 202, p. 18-27. https://doi.org/10.1016/j.rse.2017.06.031
Grunert, J., Lehmkuhl, F., Walther, M. 2000. Paleoclimatic evolution of the Uvs Nuur basin and adjacent areas (Western Mongolia). Quaternary International, vol. 65-66, p. 171-192. https://doi.org/10.1016/S1040-6182(99)00043-9
Hack, J.T. 1973. Stream-profile analysis and stream-gradient index. Journal Research of the United States Geological Survey, vol. 1, p. 421-429.
Hagg, W., Braun, L.N., Kuhn, M., Nesgaard, T.I.

2007. Modelling of hydrological response to climate change in glacierized Central Asian catchments. Journal of Hydrology, vol. 332(1-2), p. 40-53. https://doi.org/10.1016/j.jhydrol.2006.06.021
Harrison, S.P., Yu, G., Tarasov, P.E. 1996. Late Quaternary lake-level record from northern Eurasia. Quaternary Research, vol. 45(2), p. 138-159. https://doi.org/10.1006/qres.1996.0016
Hassen, M.B., Deffontaines, B., Turki, M.M. 2014. Recent tectonic activity of the Gafsa fault through morphometric analysis: Southern Atlas of Tunisia. Quaternary International, vol. 338, p. 99-112. https://doi.org/10.1016/j.quaint.2014.05.009
Herzschuh, U. 2006. Palaeo-moisture evolution in monsoonal Central Asia during the last 50,000 years. Quaternary Science Reviews, vol. 25(1-2), p. 163-178. https://doi.org/10.1016/j.quascirev.2005.02.006
Huete, A., Didan, K., Miura, T., Rodriguez, E.P., Gao, X., Ferreira, L.G. 2002. Overview of the radiometric and biophysical performance of the MODIS vegetation indices. Remote Sensing of Environment, vol. 83(1-2), p. 195-213. https://doi.org/10.1016/S0034-4257(02)00096-2
Jasechko, S., Sharp, Z.D., Gibson, J.J., Birks, S.J., Yi, Y., Fawcett, P.J. 2013. Terrestrial water fluxes dominated by transpiration. Nature, vol. 496(7445), p. 347-350. https://doi.org/10.1038/nature11983
Jigj, S. 1975. Fundamental characteristics of Mongolia's relief. Ulaanbaatar: State Publishing House. (in Mongolian)
Jolivet, M., Arzhannikova, A., Frolov, A., Arzhannikov, S., Kulagina, N., Akulova, V., Vassallo, R. 2017. Late Jurassic-early Cretaceous paleoenvironmental evolution of the Transbaikal basins (SE Siberia): implications for the Mongol-Okhotsk orogeny. Bulletin de la Société Géologique de France, vol. 188(1-2), 9. https://doi.org/10.1051/bsgf/2017010
Keller, E.A., Pinter, N. 2002. Active Tectonics, Earthquakes, Uplift and Landscape. 2nd Edition, Prentice Hall, 362 p.
Kepezhinskas, V.V. 1979. Cenozoic alkaline basalts of Mongolia and their deep inclusions. Transactions of the Joint Soviet-Mongolian Scientific-Research Geological Expedition, p. 35-88. Nedra, Moscow (in Russian).
Khukhuudei, U., Kusky, T., Windley, B.F., Otgonbayar, O., Wang, L., Nie, J., Xiao, W., Zhang, L., Song, X. 2024. Cenozoic intracontinental tectonics of Mongolia and its climate effects: A synthesized review. Earth-Science Reviews, vol. 258, 104934. https://doi.org/10.1016/j.earscirev.2024.104934
Klinge, M., Schluetz, F., Zander, A., Huelle, D., Batkhishig, O., Lehmkuhl, F. 2021. Late Pleistocene lake level, glaciation, and climate change in the Mongolian Altai deduced from sedimentological and palynological archives. Quaternary Research, vol. 99, p. 168-189. https://doi.org/10.1017/qua.2020.67
Kumar, N., Dumka, R.K., Mohan, K., Chopra, S. 2022. Relative active tectonics evaluation using geomorphic and drainage indices, in Dadra and Nagar Haveli, western India. Geodesy and Geodynamics, vol. 13(3), p. 219-229. https://doi.org/10.1016/j.geog.2022.01.001
Larson, P.H., Dorn, R.I., Skotnicki, S.J., Seong, Y.B., Jeong, A., DePonty, J. 2020. Impact of drainage integration on basin geomorphology and landform evolution: A case study along the Salt and Verde rivers, Sonoran Desert, USA. Geomorphology, vol. 371, 107439. https://doi.org/10.1016/j.geomorph.2020.107439
Lehmkuhl, F., Lang, A. 2001. Geomorphological investigations and luminescence dating in the southern part of the Khangay and the Valley of the Gobi Lakes (Central Mongolia). Journal of Quaternary Science, vol. 16(1), p. 69-87. https://doi.org/10.1002/1099-1417(200101)16:1%3C69::AID-JQS583%3E3.0.CO;2-O
Li, H., Liu, X., Herzschuh, U., Cao, X., Yu, Z., Wang, Y. 2019. Vegetation and climate changes since the middle MIS 3 inferred from a Wulagai Lake pollen record, Inner Mongolia, Northeastern China. Review of Palaeobotany and Palynology, vol. 262, p. 44-51. https://doi.org/10.1016/j.revpalbo.2018.12.006
Liu, J., Zhang, Q., Singh, V.P., Song, C., Zhang, Y., Sun, P., Gu, X. 2018. Hydrological effects of climate variability and vegetation dynamics on annual fluvial water balance in large global

river basins. Hydrology and Earth System Sciences, vol. 22(7), p. 4047-4060. https://doi.org/10.5194/hess-22-4047-2018

Makrari, S., Sharma, G., Taloor, A.K., Singh, M.S., Sarma, K.K., Aggarwal, S.P. 2022. Assessment of the geomorphic indices in relation to tectonics along selected sectors of Borpani River Basin, Assam using Cartosat DEM data. Geosystems and Geoenvironment, vol. 1(3), 100068. https://doi.org/10.1016/j.geogeo.2022.100068

Marinov, N.A., Khasin, R.A. 1954. Some issues of the geomorphology of Eastern Mongolia. Voprosy Geografii, vol. 35, p. 253-259 (in Russian).

Mu, Q., Zhao, M., Running, S.W. 2011. Improvements to a MODIS Global Terrestrial Evapotranspiration Algorithm. Remote Sensing of Environment, vol. 115(8), p. 1781-1800. https://doi.org/10.1016/j.rse.2011.02.019

Murzaev, E.M. 1952. Mongolian People's Republic: Physical-geographical description. Moscow, p. 156-171. (in Russian)

National Atlas of Mongolia. 2009. Dorjgotov, D. (Ed.), Institute of Geography, Mongolian Academy of Sciences, scale 1:5,000,000.

National Atlas of Mongolia. 2022. Dorjgotov, D. (Ed.), Institute of Geography and Geoecology, Mongolian Academy of Sciences, scale 1:5,000,000

National Atlas of the Mongolian People's Republic. 1990. Academy of Sciences of Mongolia and Academy of Sciences of USSR. Ulaanbaatar and Moscow.

Natsagdorj, L., Gomboluudev, P. 2017. Climate change, desertification, and permafrost in Mongolia. In: Nyamdavaa, G. (Ed.), Environment of Mongolia, Volume I. Ministry of Environment and Tourism, Ulaanbaatar, Mongolia, Munkhiin Useg Publishing, p. 19-47 (in Mongolian).

Oki, T., Kanae, S. 2006. Global Hydrological Cycles and World Water Resources. Science, 313(5790), p. 1068-1072. https://doi.org/10.1126/science.1128845

Pang, Z. 2011. Discussion on the Management of the District of WULAGAI Grassland Ecological Protection and Construction. Beijing Agriculture, vol. 4, p. 145 (In Chinese)

Petrov, O.V., Shuwen, D., Kiselev, E.A., Morosov, A.F. 2016. Atlas of geological maps of Asia and adjacent areas. International project. VSEGEI Publishing House.

Pike, R.J., Evans, I.S., Hengl, T. 2009. Geomorphometry: A Brief Guide. In T.Hengl and H.I Reuter (Eds.), Geomorphometry: Concepts, Software, Applications. Developments in Soil Science, vol. 33, p. 1-28. https://doi.org/10.1016/S0166-2481(08)00001-9

Schumm, S.A. 1977. The Fluvial System. New York: Wiley.

Shi, Y., Liu, X., Li, B., Yao, T., 1999. A very strong summer monsoon event during 30-40 kaBP in the Qinghai-Xizang (Tibet) Plateau and its relation to precessional cycle. Chinese Science Bulletin, vol. 44, p. 1851-1858. https://doi.org/10.1007/BF02886339

Shi, Y., Yu, G., Liu, X., Li, B., Yao, T. 2001. Reconstruction of the 30-40 ka BP enhanced Indian monsoon climate based on geological records from the Tibetan Plateau. Palaeogeography, Palaeoclimatology, Palaeoecology, vol. 169(1-2), p. 69-83. https://doi.org/10.1016/S0031-0182(01)00216-4

Sorg, A., Bolch, T., Stoffel, M., Solomina, O., Beniston, M. 2012. Climate change impacts on glaciers and runoff in the Tien Shan (Central Asia). Nature Climate Change, vol. 2(10), p. 725-731. https://doi.org/10.1038/nclimate1592

Strahler, A.N. 1952. Hypsometric (area-altitude) analysis of erosional topography. GSA Bulletin, vol. 63(11), p. 1117-1142. https://doi.org/10.1130/0016-7606(1952)63[1117:HAAOET]2.0.CO;2

Syrnev, I.P. 1982. Ancient valleys of the Eastern Mongolian plains. Geomorphology, vol. 3, p. 69-74 (in Russian)

Tarasov, P., Dorofeyuk, N., Tseva, E.M. 2000. Holocene vegetation and climate changes in Hoton-Nur basin, northwest Mongolia. Boreas, vol. 29(2), p. 117-126. https://doi.org/10.1111/j.1502-3885.2000.tb01205.x

Tarboton, D.G. 1997. A New Method for the Determination of Flow Directions and Contributing Areas in Grid Digital Elevation Models. Water Resources Research, vol. 33(2), p. 309-319. https://doi.org/10.1029/96WR03137

Tomurtogoo, O. 2012. Tectonic subdivision of

Mongolian orogenic belts. Khaiguulchin, vol. 46, p. 20-35 (in Mongolian)

Tomurtogoo, O., Byamba, J., Badarch, G., Minjin, Ch., Orolmaa, D., Khosbayar, P., Chuluun, D. 1998. Geologic map of Mongolia at the scale of 1:1 000 000 and Summary (explanatory notes of the map). Mineral Resources Authority of Mongolia, Ulaanbaatar.

Tomurtogoo, O., Windley, B.F., Kroner, A., Badarch, G., Liu, D.Y. 2005. Zircon age and occurrence of the Adaatsag ophiolite and Muron shear zone, central Mongolia: constraints on the evolution of the Mongol-Okhotsk ocean, suture and orogen. Journal of the Geological Society, vol. 162(1), p. 125-134. https://doi.org/10.1144/0016-764903-146

Tsegmid, Sh. (Ed.). 1969. Physical Geography of Mongolia. Ulaanbaatar: State Publishing House. (in Mongolian)

Tucker, C.J. 1979. Red and photographic infrared linear combinations for monitoring vegetation. Remote Sensing of Environment, vol. 8(2), p. 127-150. https://doi.org/10.1016/0034-4257(79)90013-0

Ulambadrakh, K. 2015. Morphological origin of the Eastern Mongolian Plain. Haiguulchin Journal, vol. 54, p. 91-107 (in Mongolian)

Vlodavets, V.I. 1950. The Dariganga volcanic region. Doklady of the USSR Academy of Sciences, New Series, vol. 72(5), p. 933-935 (in Russian)

Wan, Z., Hook, S., Hulley, G. 2015. MOD11A1 MODIS/Terra Land Surface Temperature/ Emissivity Daily L3 Global 1km SIN Grid V006. NASA EOSDIS Land Processes DAAC. https://doi.org/10.5067/MODIS/MOD11A1.061

Wang, T., Tong, Y., Xiao, W., Guo, L., Windley, B., Donskaya, T., Li, S., Tserendash, N., Zhang, J. 2022. Rollback, scissor-like closure of the Mongol-Okhotsk Ocean and formation of an orocline: magmatic migration based on a large archive of age data. National Science Review, vol. 9(5), p. nwab210. https://doi.org/10.1093/nsr/nwab210

Willgoose, G., Hancock, G. 1998. Revisiting the hypsometric curve as an indicator of form and process in transport-limited catchment. Earth Surface Processes and Landforms, vol. 23(7), p. 611-623. https://doi.org/10.1002/(SICI)1096-9837(199807)23:7<611::AID-ESP872>3.0.CO;2-Y

Yembuu, B. (Ed.). 2021. The Physical Geography of Mongolia. Geography of the Physical Environment, Springer Cham, 218 p. https://doi.org/10.1007/978-3-030-61434-8

Zhou, Y., Batelaan, O., Guan, H., Liu, T., Duan, L., Wang, Y., Li, X. 2024. Assessing long-term trends in vegetation cover change in the Xilin River Basin: Potential for monitoring grassland degradation and restoration. Journal of Environmental Management, vol. 349, 119579. https://doi.org/10.1016/j.jenvman.2023.119579